Chapter 8
Heat-Treated Non-precious-Metal-Based Catalysts for Oxygen Reduction

Lior Elbaz, Gang Wu, and Piotr Zelenay

Abstract Non-precious metal catalysts have shown good activity towards oxygen reduction reaction, both in basic and acidic media. The use of NPMCs in fuel cells and metal–air batteries has been hampered by two main issues: the synthesis complexity, translating into a high fabrication cost, and by relatively low stability when compared to platinum-based catalysts, especially in acidic media. In order to overcome these issues, a new class of non-precious metal oxygen reduction catalysts was developed that involves heat treatment as a key step in the NPMC synthesis. This chapter provides a review of the progress in research on heat-treated non-precious metal catalysts of oxygen reduction since the early 1970s until today. The focus of this chapter is on the activity and morphology of the state-of-the-art heat-treated ORR catalysts and trends in the development of more active and durable materials.

8.1 Introduction

Since the discovery of their ability to catalyze the oxygen reduction reaction (ORR) [1] and up until today, there has been a continuous growth in the interest in macrocyclic compounds as reviewed in the Chap. 7 of this book. Researchers in various fields, from biology to physics and chemistry, have investigated the ORR mechanism and modified the macrocyclic structures to achieve better catalytic performance [2]. While very good catalytic activity was demonstrated under certain conditions [3, 4], mainly at room temperature and in neutral environment, the lack of stability under harsher acidic conditions and at elevated temperatures have made non-precious metal catalysts (NPMCs) for oxygen reduction less attractive for prominent technologies, such as fuel cells, in particular for the polymer electrolyte fuel cells (PEFCs) operating under acidic conditions (pH $<$ 1) and at an average temperature of 80 °C.

L. Elbaz • G. Wu • P. Zelenay (✉)
Los Alamos National Laboratory, Los Alamos, NM 87545, USA
e-mail: zelenay@lanl.gov

M. Shao (ed.), *Electrocatalysis in Fuel Cells*, Lecture Notes in Energy 9,
DOI 10.1007/978-1-4471-4911-8_8,

In the case of macrocyclic compounds, such as porphyrins and phthalocyanines, it was concluded that the catalytic ORR sites are the transition metal themselves [5]. It was shown by Jahnke et al. that there is a clear dependence between the type of the metal center and the catalytic activity [1]. The stability of catalysts in this group depends on their ability to maintain their macrocyclic character. That character can be compromised in a reaction with a hydrogen peroxide, an intermediate product of ORR in acidic environment, which is capable of oxidizing and splitting the macrocyclic structure [6]. The stability of this family of catalysts also depends on their ability to resist the dissociation of the transition metal. Metals tend to easily dissociate in their reduced form, resulting in an inactive, protonated, metal-free macrocycle [7]. On top of these inherent stability issues, metalloporphyrins and metallo-phthalocyanines, especially the analogous biomimetic ones [8], are considered to be extremely hard to make because of a high number of the synthesis steps required. This translates into high manufacturing cost, outweighing the benefit of the low initial materials cost.

Over time, many variations of macrocyclic compounds were introduced in order to enhance catalytic activity and stability [9]. One of the more prominent paths taken in the design of such catalysts was based on heat-treating porphyrins and phthalocyanines. The work on heat-treated macrocyclic compounds started in the early 1970s by Jahnke et al. [10] and was followed by the work of Bagotzky [11] and by Wiesner and Fuhrmann [12, 13]. All three groups sought to activate phthalocyanines and porphyrins for oxygen reduction and showed improvements in both the activity and durability of catalysts following the heat treatment. Since then, the work on heat-treated non-precious-metal-based ORR catalysts has progressed in parallel to the research on non-heat-treated metallo-macrocyclic compounds and other transition metal complexes. While the heat treatment of these complexes was shown to increase the activity and stability of catalysts, it also resulted in a loss of their original structure [14] and formation of materials with new, usually poorly defined morphology, the nature of which typically depends on the heat-treatment temperature [15], gas atmosphere [16], and the type of carbon support used [17]. Those significant changes raised fundamental questions regarding the final catalyst structure and the nature of the active site, the two key parameters for the design of future catalysts.

In their extensive work, Jahnke et al. used different chelates to coordinate Co, Mn, Fe, Cu, and Ni. They showed that the most durable ORR catalysts involve $Co–N_4$ complexes [10]. In order to find inexpensive alternatives to the macrocyclic compounds, various research groups studied the synthesis routes for heat-treated transition metal complexes using less complex ligands, such as polyacrylonitrile [18], tetraazaannulene [19], and phenanthroline [20]. A significant breakthrough was made in the early 2000s by Dodelet et al. who were able to increase the activity of Fe–N–C compounds using two heat-treatment steps at different temperatures and in different gases [21]. While this new category of NPMCs showed ORR activity comparable to that of Pt-based catalysts, it lacked the durability of Pt [22], which became the main challenge for non-precious metal catalysts for oxygen reduction.

8.2 Heat-Treated Macrocyclic Compounds

Heat treatment of macrocyclic compounds was shown to dramatically increase their ORR catalytic properties. The important factors in the heat treatment of catalysts will be discussed in this section together with their effect on the ORR catalysis. Also discussed will be the catalyst structure. The majority of research in this field has focused on the macrocyclic complexes of transition metals, heat-treated in the presence of various carbons. That class of ORR catalysts will be addressed below.

8.2.1 Heat Treatment

8.2.1.1 Conditions

Throughout the years, the heat-treatment conditions for macrocyclic compounds were one of the most extensively studied parameters of NPMC synthesis. It was argued that the right selection of heat-treatment conditions could lead to significant improvements to both the activity and durability of resulting materials. In their first publication on heat-treated transition metal complexes, Jahnke et al. concluded that of the studied ligands (N_2, N_4, O_2, O_4, S_2, and S_4), N_4-ligand containing precursors, e.g., porphyrins and phthalocyanines, are most efficient in inducing the ORR activity [10]. Jahnke et al., as well as other authors, continued that research focusing predominantly on the optimization of heat-treatment conditions for macrocyclic compounds. The most important conditions included the following:

1. Temperature
2. Gas atmosphere
3. Duration

The temperature range used to heat-treat the precursors was at first relatively wide, from 300 to 1,000 °C. Wiesener et al. studied the effect of heat-treatment temperature on the ORR current density at catalysts derived from N_4 macrocycles at a potential of 0.70 V (vs. RHE) in 2.25 M H_2SO_4 (Fig. 8.1) [23]. They found that the optimum temperature for heat-treating cobalt tetraazaannulene (CoTAA) on activated carbons P33 and P33p was around 650 °C.

From that and other published work, it can be concluded that the optimum heat-treatment temperature (from 600 to 800 °C for macrocyclic compounds) and heat-treatment duration are highly dependent on the structure of the precursor and the nature of the transition metal. It can also be concluded that iron-based catalysts require higher temperature to achieve their maximum performance compared to cobalt-based catalysts with the same ligand.

The optimum heat-treatment temperatures to reach best ORR durability and optimum activity of NPMCs were found not to be the same, especially under acidic conditions. Maximum durability tends to be reached following heat treatment at temperatures by up to 300 °C higher than the temperatures yielding catalysts with the highest activity [23].

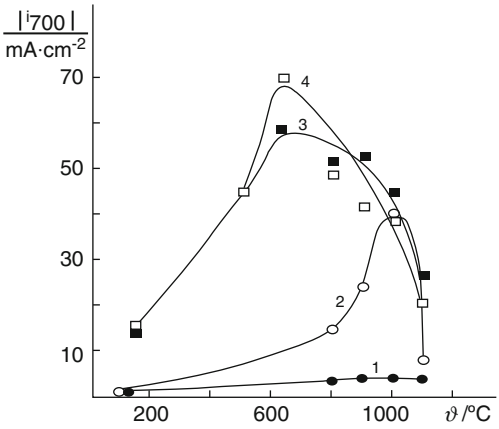

Fig. 8.1 Influence of the heat-treatment temperature on the ORR current at chelate-modified carbon electrodes measured at 0.70 V (vs. RHE). (1) H_2TAA on P33p-carbon support, (2) H_2TAA on P33-carbon support, (3) CoAA on P33p, and (4) CoTAA on P33. Heating rate 4 K min^{-1} (reprinted with permission from the *Journal of Electroanalytical Chemistry* [24])

The effect of the gaseous atmosphere was studied by Tarasevich and Radyuskina who concluded that under N_2, Ar, and He in the temperature range of 500–1,000 °C for different dwell times between 0.3 and 5.0 h, the activity and durability of the studied metalloporphyrins and metallo-phthalocyanines were similar [25]. This was a case for disagreement between different groups who observed dependence between the activity of heat-treated catalysts and the gas used during the heat treatment. For example, Dhar et al. showed the difference in the catalytic activity of heat-treated CoTAA under vacuum, N_2, Ar, and N [26]. They concluded that the most active ORR catalyst was obtained under vacuum with the following decrease in activity: vacuum $>$ N_2 $>$ Ar $>$ N (Fig. 8.2). Dodelet and his collaborators [27] showed that an iron tetra(methoxyphenyl) porphyrin is the most stable, but the least active when heat-treated in Ar, and that it becomes very active and loses its stability when treated in ammonia, an effect attributed to the concurrent increase in the microporous surface area, as well as the N and Fe surface content. The authors raised important questions about the catalyst design and optimum heat-treatment conditions for maximum stability and activity.

It can be concluded that the importance of the gas used during the synthesis is highly dependent on the type of precursor and carbon support employed in the heat treatment.

8.2.1.2 Precursors

One of the most important factors affecting the activity of non-heat-treated transition metal macrocyclic complexes is their structure, more specifically, the ligand, the substituents, and the metal center [28]. The role of those factors closely ties to the mechanism by which the complexes are activated and bind oxygen.

Although metallo-macrocycles are generally unlikely to maintain their original structure after the heat treatment [29], that original structure before the treatment is important as it often affects final distribution of atoms in the catalysts and its

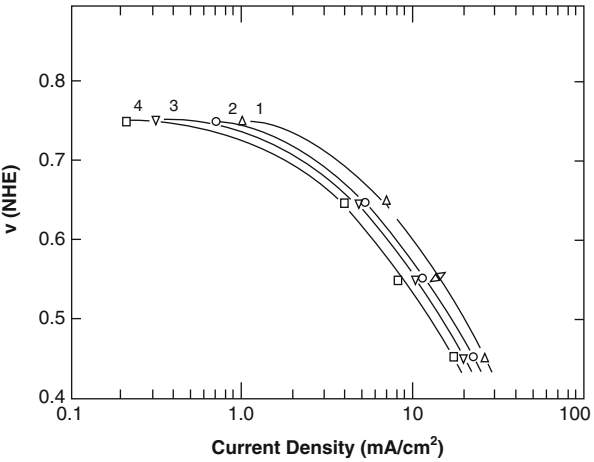

Fig. 8.2 Steady-state current-potential curves in 4 N H_2SO_4 for adsorbed $CoTAABr_2$ on acetylene-black carbon, heat-treated at 500 °C for 30 min in various atmospheres: (1) vacuum, (2) nitrogen, (3) argon, and (4) nitrogen passed over heated Cu (reprinted with permission from *Electrochimica Acta* [26])

interaction with the carbon support. Van Veen et al. [30] studied 15 different porphyrins and phthalocyanines containing various metal centers and metal-free macrocycles (Fig. 8.3). Other nitrogen precursors, such as phthalocyanine/phenolic resin [31], aminoantipyrine [32], and corrole [33], have been explored in the NPMCs synthesis, showing improved activity and durability for the ORR. From those studies, it appears that heat-treating selected macrocycles improve their ORR catalytic activity and that substituent-dependent ORR activity trends are identical before and after the treatment regardless of the metal center. In general, the governing factors that apply to non-heat-treated transition metal macrocycles discussed in the previous chapter also apply to the heat-treated macrocyclic precursors in this chapter.

8.2.1.3 Metal Center

The ORR performance of NPMCs strongly depends on the transition metal used. In their extensive research, which included 9 metallo-phthalocyanines and 24 metal chelates, Beck et al. demonstrated very strong dependence of the ORR activity on the metal center [34]. The authors concluded that the activity of transition metal complexes decreases in the following order: Fe > Co > Ni > Cu ≅ Mn. In general, a consensus has by now been reached in the non-precious metal research community that iron and cobalt yield the most ORR-active catalysts among transition-metal-based macrocyclic compounds. Alt et al. explained that dependence using the molecular orbital (MO) theory [35]. They found that the d_z^2 orbital of the metal ion is most likely to bind the oxygen molecule and that an empty d_z^2 orbital favors the partial electron transition from the metal to the antibonding π* orbitals of the oxygen during the formation of a chelate–oxygen complex. Thus, the emptier the

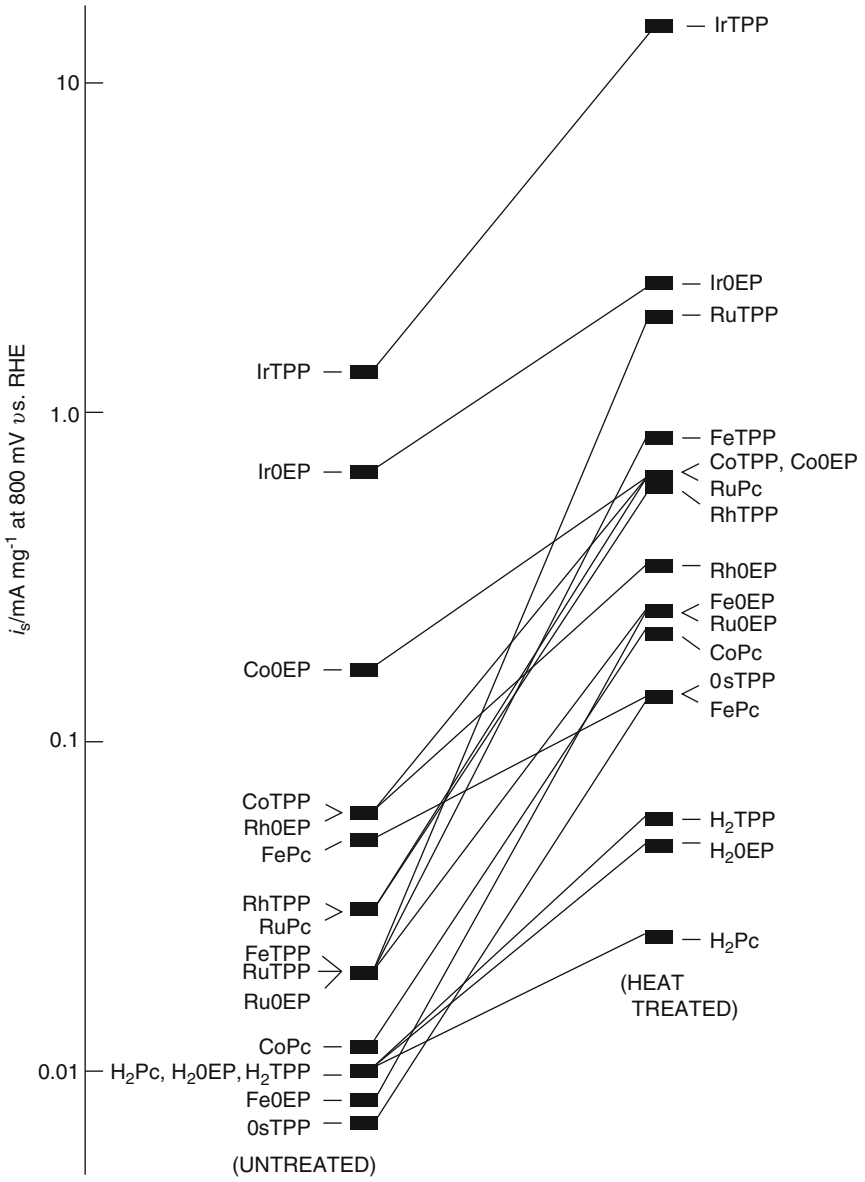

Fig. 8.3 ORR activity of various porphyrins and phthalocyanines before and after heat treatment in an inert gas atmosphere (reprinted with permission from the *Journal of the Chemical Society, Faraday Transactions I* [30])

d_z^2 orbital is, the more active is the transition metal complex in the ORR. The latter conclusion supports findings of the aforementioned study by Beck et al. Similar trends and explanation appear to hold true for heat-treated transition metal complexes [29].

8.2.2 Structure of Heat-Treated Macrocyclic ORR Catalysts

Although factors governing the synthesis of active and durable heat-treated NPMCs have been well documented in the scientific literature, the final catalyst structure is still not entirely understood, mainly due to the fact that most catalysts are synthesized in the presence of different carbon supports.

The presence of carbon makes it difficult to obtain a clear picture of the molecular structure of heat-treated macrocyclic compounds, even when the most sophisticated techniques are used. Van Veen et al. studied the structure of heat-treated transition metal macrocycles on carbon supports by a wide range of techniques, including Fourier transform infrared (FTIR), electron spin resonance spectroscopy (ESR), Mössbauer spectroscopy, X-ray photoelectron spectroscopy (XPS), extended X-ray absorption fine structure spectroscopy (EXAFS), X-ray diffraction (XRD), transmission electron microscopy (TEM), differential thermal analysis (DTA), thermogravimetric analysis (TGA), and mass spectroscopy [36, 37]. They found that the heat treatment leads to the formation of isolated metal sites in an axially symmetric environment, presumably created by the thermally modified ligand. These results led to a conclusion that thermal treatment does not cause the formation of catalytically active metallic particles. The results of that study also provided support for Fuhrhop's observation of a surface complex originating in a reaction between radicals formed at the metal complex and the carbon support [38]. Van Veen et al. postulated that during the decomposition of complexes in this family of compounds in the temperature range of 300–1,000 °C, the first part of the complex to react with the carbon surface are the ligand substituents, followed by the reaction of the rest of the macrocycle with the carbon support at higher temperatures (with the inner ring of the macrocycle postulated to retain some of its original structure). This leads to the formation of a range of surface complexes responsible for a continuous increase in stability with increasing temperature of the heat treatment.

Vallejos-Burgos et al. studied the structure and activity of a free-base phthalocyanine, Cu phthalocyanine, and Co phthalocyanine after heat-treating the compounds at different temperatures [39]. The structural changes that occurred during the heat treatment are summarized in Fig. 8.4. It is clear from that study that the structural evolution of the macrocycle and carbon support associated with a loss of nitrogen or changes in the microporosity of the support depend on the metal center.

A summary of the interesting research by Wiesener et al. on the loss of nitrogen at different heat-treatment temperatures is given in Table 8.1 [13, 24]. The authors observed a gradual decrease in the nitrogen mass in the catalysts with an increase in the heat-treatment temperature, from 3.05 wt% in the original sample to 1.05 wt% after the short-time heat treatment at 1,000 °C. The loss of nitrogen at 1,000 °C correlates well with a significant decrease in the ORR activity of the catalyst.

Many hypothetical structures of the heat-treated macrocyclic compounds have been proposed in the electrocatalysis literature to date. Most of those structures involve the formation of a covalent bond between the macrocycle and the carbon

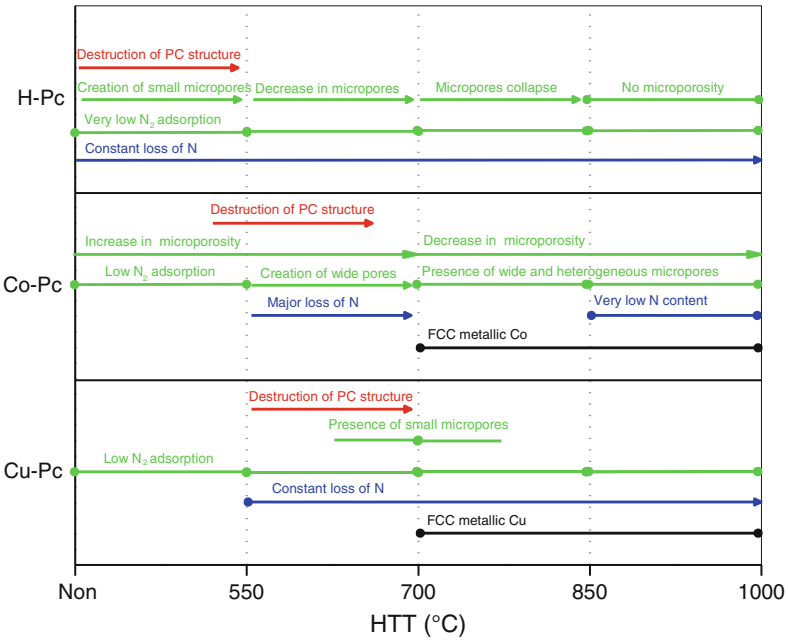

Fig. 8.4 A schematic representation of main structural changes occurring during the heat treatment of various phthalocyanine samples (reproduced from *Fuel* [39])

Table 8.1 Nitrogen content of heat-treated Co(II) dibenzotetraazaannulene on active carbon P33 [24]

Heat-treatment temperature (°C)	Heat-treatment time (h)	Nitrogen mass (%)
None	–	3.05
400	5	2.9
450	5	2.5
500	5	2.4
560	5	2.2
630	5	2.2
700	5	2.1
1,000	Short term	1.05

support [40]. In some cases it was shown that a portion of the macrocycle is imbedded in the support (Fig. 8.5) [41].

The real structure, or structures, of heat-treated ORR catalysts is yet to be revealed. The catalyst makeup is likely to strongly depend on the precursors used, with the structure of catalysts derived from different macrocycle compounds differing from one another due to such factors as the type of a macrocycle, substituent, carbon support, and the metal center. This is an intriguing subject of future research that promises to produce non-precious metal ORR catalysts with much improved activity and performance durability.

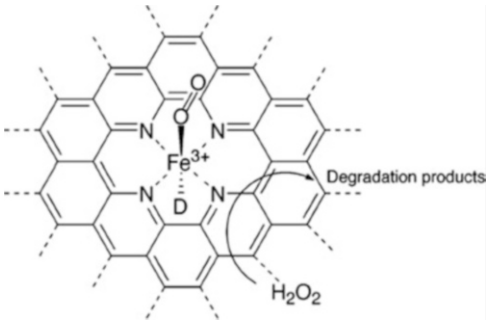

Fig. 8.5 Proposed model structure of the active site and ORR catalysis mechanism after a heat treatment of Fe tetramethoxyphenylporphyrin (FeTMPP) on a Black Pearls® support at 900 °C in Ar (reprinted with permission from the *Journal of Physical Chemistry B* [41])

8.3 Heat-Treated Non-macrocyclic Catalysts for ORR

In spite of a very significant progress achieved with heat-treated macrocyclic compounds as ORR catalysts since the early 1970s, the activity and durability of that family of catalysts are still insufficient for replacing platinum at the fuel cell cathode and in other applications. Furthermore, the complex structure of macrocyclic compounds makes their synthesis expensive and potentially noncompetitive with precious-metal-based catalysts also from the materials cost point of view. For those reasons, much effort has been invested by the electrocatalysis research community in recent years into finding less expensive and catalytically more active non-precious metal ORR catalysts that would not rely on macrocylic compounds as either catalysts or catalyst precursors. In the past decade, there has been a significant improvement both in the activity and of non-macrocyclic catalysts, expected to be manufactured at a fraction of the cost of their macrocyclic counterparts. In this section, we review the precursors, synthesis routes, and applications of this relatively new family of catalysts.

8.3.1 Precursors

Heat-treated transition metal–nitrogen–carbon (M–N–C) NPMCs can be divided into three main groups: (1) catalysts obtained from transition-metal-based macrocycles (discussed above); (2) catalysts derived from metal salts and gaseous nitrogen precursors, such as NH_3; and (3) catalysts synthesized from inorganic metal salts and simple nitrogen-containing molecules [42]. In this section, we will focus on NPMCs from group 3. This group of catalysts has received much attention since 2006, evidenced by a high number of published papers (Fig. 8.6).

Even though the heat treatment of virtually any mixture of nitrogen, metal, and carbon species can yield a material with some ORR activity, the selection of precursors, supports, and synthesis conditions plays a major role in obtaining materials with high activity and long-term durability required of practical catalysts [43, 44].

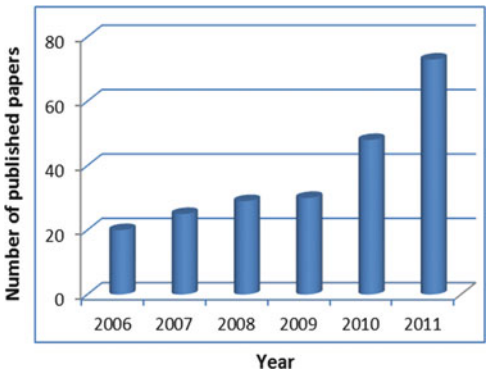

Fig. 8.6 Published papers associated with group 3 NPMCs from 2006 to 2011

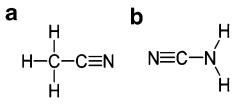

Fig. 8.7 Molecular structure of (**a**) acetonitrile and (**b**) cyanamide

8.3.1.1 Nitrogen Precursors

According to previous research on nitrogen-doped carbons heat-treated at temperatures above 700 °C [45, 46], nitrogen atoms can replace atoms in the carbon lattice. It has been generally recognized that nitrogen-doped sites in graphitic carbon layers can act as reactive centers and enhance the ORR due to favorable morphology modification and high electron density induced by the nitrogen. The catalytic properties of doped N–C structures in M–N–C catalysts were found to be tunable through varying the catalyst synthesis conditions [43, 47]. In particular, nitrogen precursors used in the synthesis were found to be crucial to the formation of catalyst nanostructures. In this part, we divide nitrogen precursors into three different groups: (1) C≡N-based nonaromatic precursors, (2) C-N-based nonaromatic amine precursors, and (3) aromatic precursors.

C≡N-Based Nonaromatic Precursors

Acetonitrile and cyanamide are the most common nitrogen precursors containing C≡N bonds in the catalyst synthesis (Fig. 8.7).

Matter et al. heat-treated at 900 °C acetonitrile together with iron acetate salts supported on Vulcan [46]. The most active catalysts, containing significantly higher amount of the pyridinic nitrogen (as determined by XPS) were formed when Fe was added to the support before the heat treatment. The current-potential ORR polarization plots, obtained using 2 % Fe on Vulcan and heat-treated for 2 h at 900 °C, are shown in Fig. 8.8. Although the measured ORR activity is not as promising in this

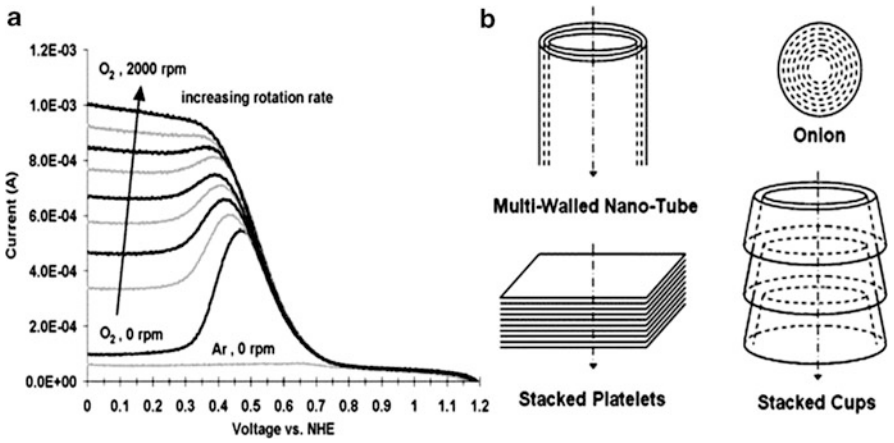

Fig. 8.8 (**a**) ORR activity of Fe catalyst derived from acetonitrile and (**b**) schematic diagrams of common carbon nanostructures demonstrating plane orientation relative to the central axis and resulting edge plane exposure (reprinted from ref. [46] with permission from Elsevier)

case as in some other cases [42], the results highlight the importance of in situ formed carbon nanostructures for the ORR active site formation. Different carbon nanostructures, such as tubes, fibers and onion-like carbon, were observed in the catalysts obtained via the decomposition of acetonitrile. The nanostructures were found to be rich in pyridinic nitrogen and exposed plane edges. As shown in Fig. 8.8, onion-like structures and tubes (especially longer ones) have mostly basal planes exposed, whereas carbon fibers with stacked platelets or cups have significant plane edge exposure. The enhanced catalytic activity of such structures is assumed to be associated with the increased plane-edge exposure in carbon nanostructures, marked by the pyridinic nitrogen.

Cyanamide (CM) was firstly explored at Los Alamos as a precursor of M–N–C oxygen reduction catalysts [48]. The most active catalyst, obtained following a heat treatment at 1,050 °C, showed very high activity relative to previously reported NPMCs, with an open circuit voltage (OCV) value of 1.0 V and a current density of 105 mA cm^{-2} at 0.80 V (*iR*-corrected) in H_2/O_2 fuel cell testing (Fig. 8.9). The reason for choosing cyanamide as a nitrogen precursor was that the compound had been known to act as precursor for graphitic C_3N_4 structures following high-temperature treatment [49]. Although the original motivation for the use of cyanamide was to increase the nitrogen content in the graphitized carbon structure, this was not the outcome. Instead, cyanamide was found to aid in the incorporation of sulfur from the iron-sulfate precursor into the carbon. It was also found that the decomposition of sulfate and evolution of SO_2 are greatly depressed in the presence of cyanamide. This was an indication that the interaction between cyanamide and sulfate (or sulfate-derived species) can stabilize sulfur in the sample, likely through

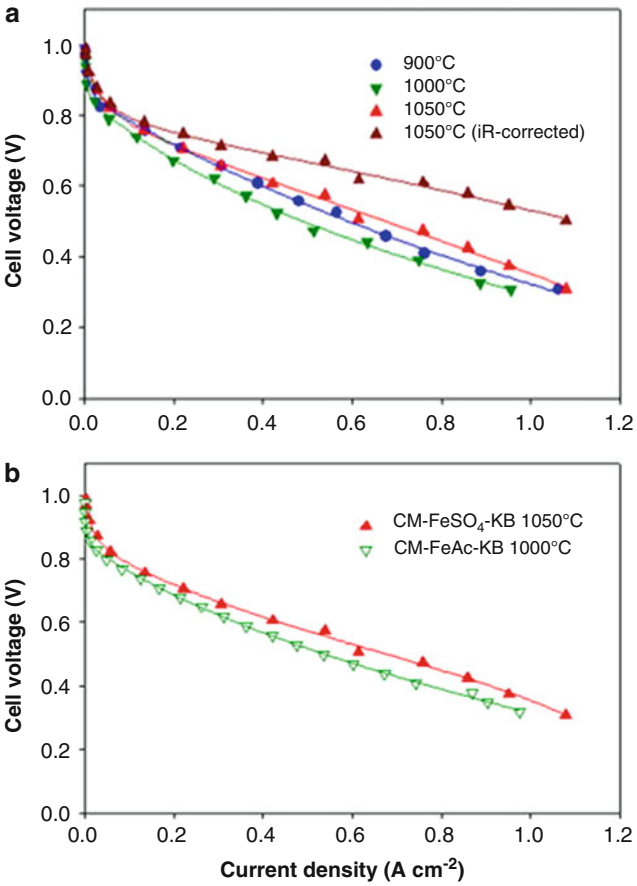

Fig. 8.9 (**a**) Fuel cell polarization plots recorded with CM–$FeSO_4$–KB ORR catalysts obtained at different heat-treatment temperatures; (**b**) fuel cell polarization plots comparison with CM–$FeSO_4$–Ketjenblack heat-treated at 1,050 °C and CM–FeAc–KB heat-treated at 1,000 °C. Nafion®117 membrane; anode: 30 psig H_2, 0.25 mg_{Pt} cm^{-2} (catalyzed cloth GDL, E-TEK); cathode: 30 psig O_2, non-precious catalyst loading 4.0 mg cm^{-2}; 100 % RH anode and cathode humidification; 300/500 standard mL per minute anode/cathode flow rates for H_2 and O_2, respectively; MEA surface area 5 cm^2 (reprinted from ref. [48] with permission from Elsevier)

the formation of C–S bonds. To further determine whether sulfur enhances the ORR activity of the CM-based catalyst, samples were prepared using Fe(II) acetate as the iron source instead of iron sulfate, thus avoiding any sulfur presence. The current density measured with these catalysts at high fuel cell voltages (> 0.8 V) was found to be about half of the value measured with the catalyst prepared using the iron-sulfate precursor (Fig. 8.9b). This difference indicates that sulfur may be responsible for the improved ORR activity of CM-based catalysts.

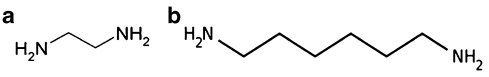

Fig. 8.10 Molecular structures of (**a**) ethylenediamine and (**b**) hexamethylenediamine

C–N-Based Nonaromatic Amine Precursors

Diamines have been one of the most efficient nitrogen precursors used in the NPMC synthesis to date due to their ability to coordinate transition metals and form complexes with four nitrogens (MN_4) [50]. The structures of ethylenediamine (EDA) and hexamethylenediamine (HDA) are shown in Fig. 8.10.

EDA has been used as a nitrogen precursor in the catalyst synthesis ever since it was first introduced by a University of South Carolina research group [50, 51]. Cobalt species were chelated by EDA, giving rise to CoN_4 structures, simpler than the traditional macrocyclic compounds. While the resulting Co–EDA catalyst exhibited improved activity compared to previous reports, it still suffered from poor four-electron selectivity [42]. It was found that a nitric-acid treatment and the resulting formation of quinone-like groups on the carbon surface were key to increasing the dispersion of the Co–EDA complex on supports by creating adsorption sites for the amine [51]. The CoFe–N chelate was then deposited on metal-free carbon-composite support leading to a catalyst with improved ORR activity and durability (Fig. 8.11) [50]. The carbon composite catalyst showed an onset potential for oxygen reduction as high as 0.87 V vs. RHE in H_2SO_4 solution and an H_2O_2 yield of less than 1 %. Current densities as high as 0.27 A cm^{-2} at 0.6 V and 2.3 A cm^{-2} at 0.2 V were demonstrated in fuel cell testing using a catalyst loading of 6.0 mg cm^{-2}. No significant performance decrease was observed for 480 h of continuous fuel cell operation. According to XPS analysis, all metal species were removed from the surface by chemical treatment in 0.5 M H_2SO_4. It was proposed that transition metals facilitate the incorporation of pyridinic and graphitic nitrogen groups into the carbon matrix during the pyrolysis, leading to the formation of catalytically active ORR sites [50].

It was found that precursors containing long hydrocarbon-chain amines resulted in higher ORR activity than short-chain precursors [45, 53]. Similarly to EDA, HDA is capable of coordinating transition metals, such as Co and Fe, to form an interlinked macromolecule. A variation in the Co-to-Fe ratio in the synthesis of the HDA-derived CoFe binary catalysts results in markedly different ORR activity and four-electron selectivity (Fig. 8.12). A binary CoFe(1:3)–N–C catalyst, synthesized with a Co-to-Fe ratio of 1:3, was found to have the most positive onset and half-wave potentials and a low hydrogen peroxide yields (2–3 %). In fuel cell testing, the binary CoFe catalyst performed noticeably better than an Fe-based catalyst, especially at fuel cell voltages lower than 0.80 V. Under these experimental conditions, the best performing catalyst was found to generate a current density of 0.05 A cm^{-2} at 0.8 V and power density as high as 0.42 W cm^{-2} [52].

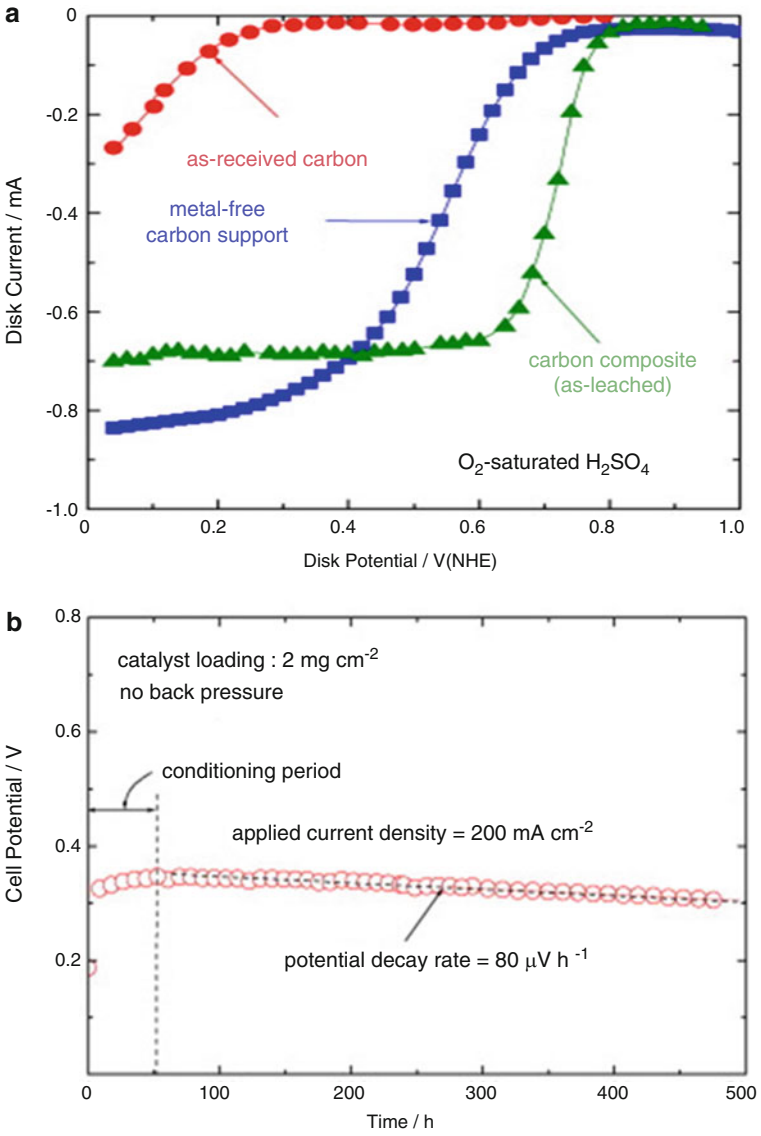

Fig. 8.11 ORR performance of an EDA-derived CoFe composite: (**a**) RDE activity in 0.5 M H_2SO_4 at room temperature and (**b**) fuel cell life tests at 80 °C at a constant current density of 200 mA cm^{-2} using H_2 and O_2 at no back pressure. Cathode catalyst loading: 2.0 mg cm^{-2} (reprinted from reference in [50] with permission from Elsevier)

Aromatic Precursors

It has long been believed that nitrogen–carbon precursors can undergo a metal-assisted graphitization during heat treatment [46]. Due to structural similarities between aromatic molecules and graphite, aromatic precursors of nitrogen have

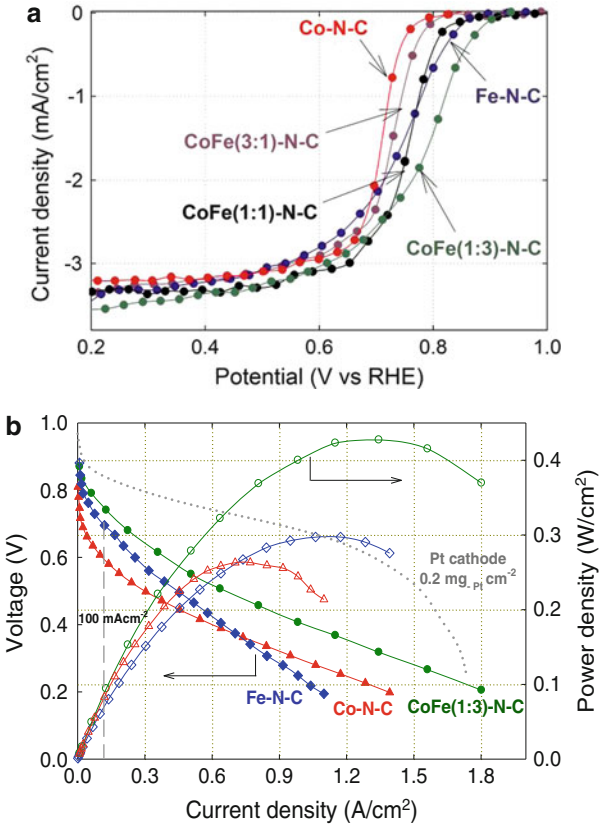

Fig. 8.12 ORR performance of CoFe–N–C NPMCs as a function of the Co-to-Fe ratio in the synthesis. (**a**) RDE measurement in 0.5 M H_2SO_4 at 25 °C and 900 rpm; catalyst loading: 0.6 mg cm^{-2}. (**b**) Fuel cell polarization plots in a H_2–O_2 cell; anode/cathode back pressure: 1.0 bar; cell temperature: 80 °C; anode: 0.25 mg_{Pt} cm^{-2}; membrane: Nafion® 212 (reprinted from ref. [52] with permission from Elsevier)

recently attracted much attention in the synthesis of NPMCs. Three aromatic precursors, nitroaniline [54], melamine [55], and polyaniline [56, 57], are shown in Fig. 8.13.

Researchers at 3M developed NPMCs by heat-treating polynitroaniline obtained via a metal-assisted polymerization of 4-nitroaniline [54]. A possible structure of the polymer derived from nitroaniline is depicted in Fig. 8.13a. The repeating unit in the polymer is quinoxaline, containing pyrazinic rather than pyridinic nitrogen [58]. The results showed that the polymerization of nitroaniline in the presence of certain anhydrous metal salts, followed by a thermal treatment, could create an NPMC with high ORR activity [54]. The nitroaniline-derived catalyst has an ORR onset potential as high as 0.94 V vs. RHE. The ORR activity is maintained throughout a broad linear Tafel region that extends over two orders of magnitude in current density, with a

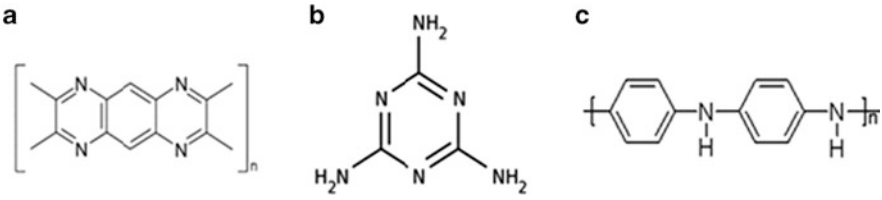

Fig. 8.13 Molecular structures for (**a**) polynitroaniline, (**b**) melamine, and (**c**) polyaniline

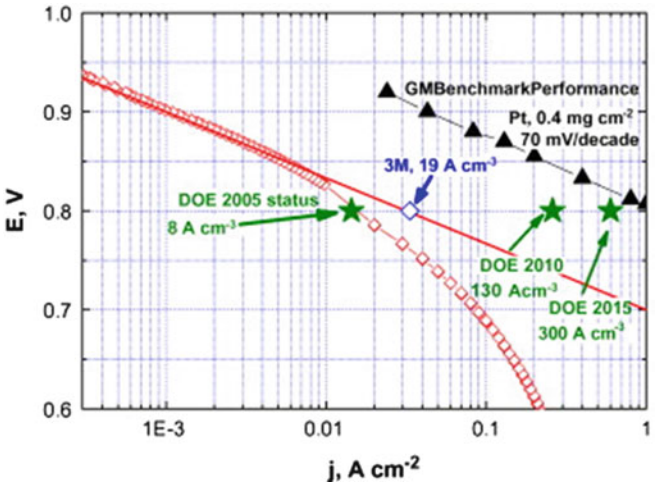

Fig. 8.14 Polarization curves of a 4-nitroaniline precursor-based catalyst. The straight-line slope is 70 mV dec^{-1}, measured at 80 °C with saturated hydrogen at the anode (180 sccm, 300 kPa backpressure) and oxygen at the cathode (335 sccm, 430 kPa backpressure) (reprinted from ref. [54] with permission from Elsevier). Pt reference catalyst data obtained from GM [59]

slope of 70 mV dec^{-1} (Fig. 8.14). The volumetric activity of the nitroaniline-derived catalyst is 19 A cm^{-3} at a fuel cell voltage of 0.8 V. Compared to macrocyclic compounds, the use of nitroaniline is a cost-effective method, amenable to scale-up. However, relatively high toxicity of nitroaniline is a drawback from the point of view of a large-scale synthesis of the catalyst.

Melamine, a trimer of cyanamide, with a 1,3,5-triazine skeleton containing 66 wt% of nitrogen, was first employed as a nitrogen precursor in NPMC synthesis by a Michigan State University group as a means of enhancing the content of doped nitrogen [55]. In a typical approach, solid melamine was ground with Ketjenblack 600JD carbon, containing adsorbed Fe(II) acetate, before it was heat-treated at 800 °C in nitrogen atmosphere. At the final stage of the synthesis, the catalyst was treated in 0.5 M sulfuric acid. The melamine-derived catalyst was found to have superior ORR activity to catalysts derived from other nitrogen precursors, such as bipyridine, pyrazine, and purine (Fig. 8.15) [55].

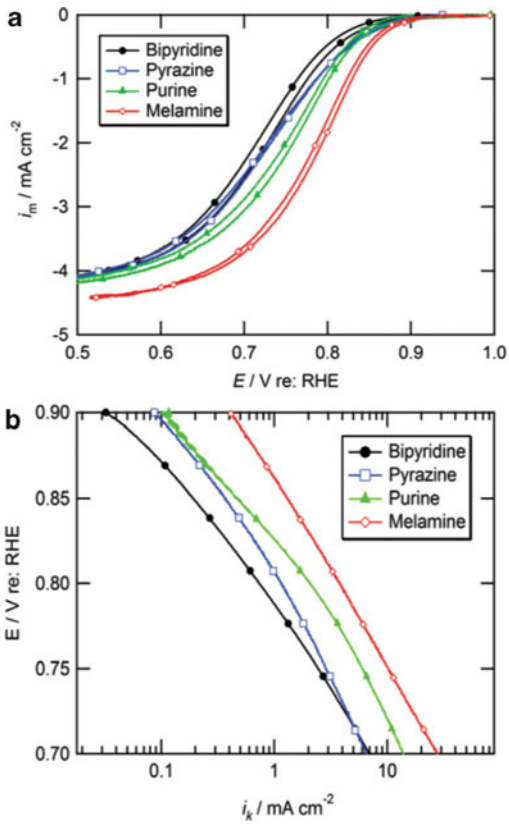

Fig. 8.15 Oxygen reduction plots at a thin-film RDE with NPMCs derived from various nitrogen precursors: (**a**) steady-state polarization plots, (**b**) *iR*- and mass-transfer corrected Tafel plots (reprinted from ref. [60] with permission from the Electrochemical Society)

The volumetric current density measured with the melamine-based catalyst was 12.4 A cm^{-3} at 0.8 V. The high ORR activity of the melamine-derived NPMC was attributed to a threefold increase in the bulk nitrogen content. It is worth noting that a 33 % increase in the BET surface area was observed for the melamine-derived catalyst relative to the bipyridine-derived catalyst, suggesting that higher surface area might have contributed to the improved ORR activity. A 50 % increase in nitrogen retention was also observed for melamine-based catalysts, compared to a bipyridine-derived catalyst. However, the direct attribution of enhanced ORR activity of the melamine-based catalyst to the total nitrogen content should be done with care in the context of findings by other authors that ORR activity is not necessarily dependent on the amount of nitrogen content in the catalyst, but rather how nitrogen is incorporated into the carbon [43, 48]. A 100-h performance durability test was performed with the melamine-based catalyst at a fuel cell voltage of 0.5 V using pure H_2 and O_2. The performance loss was less than 10 %, a respectable result by the standards of most NPMCs [55].

Recently, polyaniline (PANI), an inexpensive and nontoxic aromatic polymer, was selected as a precursor of nitrogen and carbon in the NPMC synthesis at Los Alamos [56, 57]. Because of the similarity between the structures of PANI and graphite, the heat treatment of PANI was thought to facilitate the incorporation of

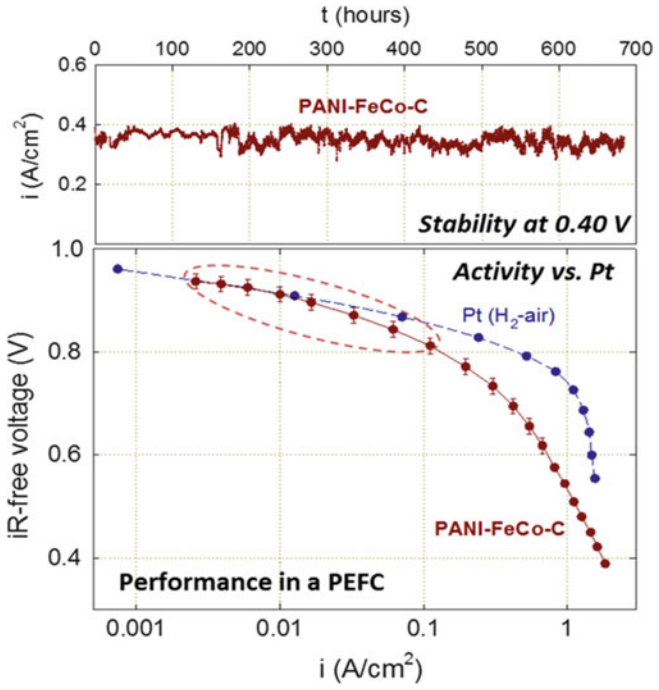

Fig. 8.16 *Bottom*: H_2–O_2 fuel cell polarization plots recorded with ~4 mg cm^{-2} of a PANI–FeCo–C catalyst in the cathode. Performance of an H_2–air fuel cell with a Pt cathode (0.2 mg_{Pt} cm^{-2}) is shown for comparison. *Top*: Long-term performance stability test of the PANI–FeCo–C catalyst in a H_2–air fuel cell at a constant fuel cell voltage of 0.40 V. Anode and cathode gas pressure 2.8 bar; anode loading 0.25 mg_{Pt} cm^{-2}; cell temperature 80 °C (reprinted from ref. [57] with permission from AAAS)

nitrogen-containing active sites into the partially graphitized carbon matrix in the presence of iron and/or cobalt. Furthermore, the use of such a polymer as a nitrogen precursor promised a more uniform distribution of nitrogen sites on the catalyst surface and possible increase in the active-site density. Heat-treated PANI-derived formulations appear to combine high ORR activity with high durability. The most active materials in the group were shown to catalyze the ORR at potentials within ~60 mV of those obtained with state-of-the-art carbon-supported Pt catalysts (Fig. 8.16) [57].

8.3.1.2 Transition Metal Precursors

While some metal-free nitrogen-doped carbon materials are at least to some degree capable of catalyzing the ORR on their own [61], an addition of transition metal(s) appears necessary for achieving high catalytic activity and improved durability of heat-treated NPMCs [62, 63]. The influence of different transition metal ions on

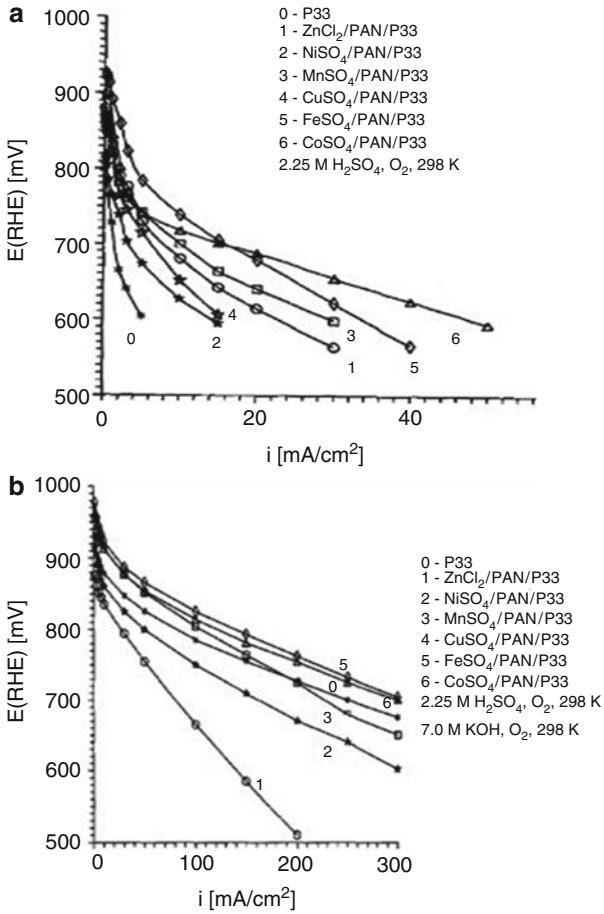

Fig. 8.17 ORR polarization for different catalysts in (**a**) 2.25 M H_2SO_4 and (**b**) 7.0 M KOH at 298 K (reprinted from ref. [64] with permission from Elsevier)

ORR activity of catalysts prepared using heat treatment of polyacrylonitrile was studied in both acid and alkaline solutions [64]. The results indicate that the nature of metallic center in the precursor plays a critical role in the ORR catalysis and can be tied to activity increase after the heat treatment. By now, there is strong experimental evidence that iron and cobalt lead to the formation of the active centers with the highest activity towards the catalysis of ORR regardless of the solution pH (Fig. 8.17). In acidic media, Fe-containing catalysts generally have more positive onset potential than Co catalysts, which suggests a higher intrinsic activity. The Fe-containing catalysts also exhibit the highest four-electron selectivity among the catalysts based on transition metals [64]. In alkaline media, Fe- and Co-based electrocatalysts often show similar activity [64].

While both Fe and Co are generally more efficient in forming active ORR sites than other non-precious metals [63], it is worth noting that the nature of the sites

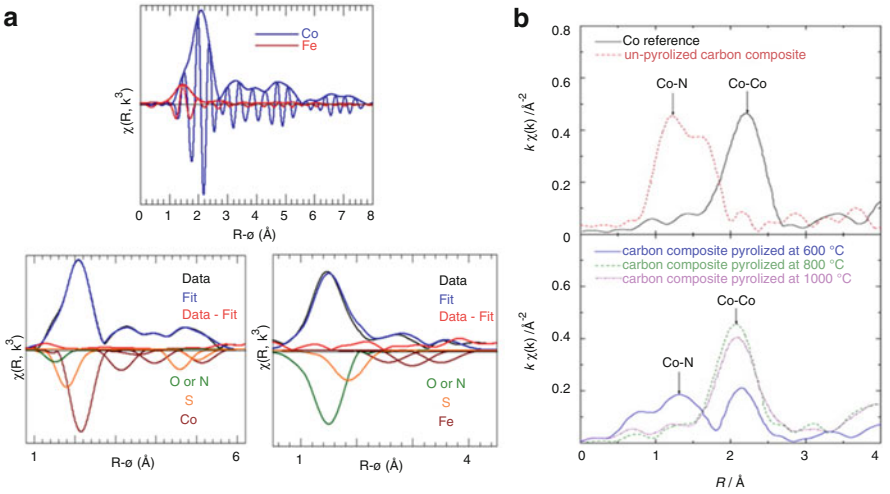

Fig. 8.18 EXAFS of (**a**) PANI–Fe–C and PANI–Co–C catalysts (reproduced from ref. [43] with permission of The Royal Society of Chemistry) and (**b**) EDA–Co–C catalyst (reprinted from ref. [50] with permission from Elsevier)

may be different for the two metals. The active sites generated in the presence of Co appear to have the onset ORR potential similar to that observed in metal-free nitrogen-doped carbon (N–C) catalysts, abundant in CN_x groups (pyridinic, quaternary nitrogens) [50]. There is strong evidence that, unlike Co-derived species, Fe directly participates in the ORR, likely via the formation of Fe–N_x type sites. Such sites have generally higher ORR activity than the metal-free sites formed in Co-based catalysts [43, 65, 66]. As follows from ex situ EXAFS studies of the coordination environment of transition metals in PANI-derived catalysts (Fig. 8.18a), the chemical environment of Fe and Co in such Fe- and Co-based catalysts is quite different. Fe–O/N coordination structures are dominant in Fe-based catalysts (signals from O and N in the local environment of the metal cannot be distinguished in EXAFS), while only small fractions of Co is bound to O/N.

In the case of EDA-derived Co catalysts (Fig. 8.18b), the EXAFS of not heat-treated sample shows the presence of one major peak around the R values of ca. 1.2 Å. That peak can be assigned the Co–N interactions. The Co–N peak weakens and the Co–Co peak becomes more apparent with an increase in the heat-treatment temperature. The CoN_x chelate complexes decompose at high heat-treatment temperatures, 800 °C and higher, which results in the formation of metallic Co species. As a consequence, the Co–N structure is no longer dominant in both heat-treated PANI- and EDA-derived Co catalysts.

Electrochemical kinetic analysis yields different Tafel slope values for Co–N–C (~59 mV dec^{-1}) and Fe–N–C (~87 mV dec^{-1}) catalysts [52, 57], attesting to different ORR mechanism in the case of the two metals. Based on the Tafel slope analysis for the ORR on Pt catalysts by Coutanceau et al. [67], the diffusion of adsorbed oxygen intermediates during the ORR is a likely the rate-determining step

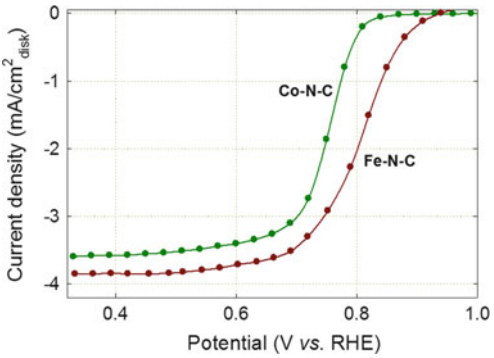

Fig. 8.19 Steady-state ORR polarization plots recorded at an RDE with PANI-derived Co- and Fe-based ORR catalysts in 0.5 M H_2SO_4 at 25 °C and at a rotation rate of 900 rpm (reproduced from ref. [43] by permission of The Royal Society of Chemistry)

on the Co–N–C catalyst. More complicated ORR mechanism on Fe–N–C catalysts is possible, involving both intermediate migration and charge transfer in the rate-determining step [68].

Regardless of the nitrogen precursor used, Fe–N–C catalysts have higher content of quaternary nitrogen compared to Co–N–C catalysts, indicating that nitrogen atoms favor doping at the interior rather than at the edges of the graphene layers in Fe-based catalysts [43, 52]. Generally, the ratio of pyridinic and quaternary nitrogens is expected to reach a steady state during the heat treatment of carbon-containing nitrogen groups [45]. The addition of Fe seems to facilitate the formation of quaternary nitrogen. The differences in the chemical and physical state of the active ORR sites are likely responsible for the lower ORR activity of the Co-based catalysts than Fe-based catalysts in acid media. The disparity in the ORR activity of PANI-derived Co- and Fe-based catalysts in the RDE testing is shown in Fig. 8.19.

Although the intrinsic activity of Co-based catalysts is lower than that of Fe-based catalysts, the use of Co usually leads to more graphitic nanostructures [43, 52], enhancing the electronic conductivity and corrosion resistance. In order to simultaneously take advantage of the apparent high ORR activity of the Fe-based catalysts and better stability of Co-based materials, binary CoFe catalysts were synthesized at Los Alamos. Enhanced activity and durability were indeed demonstrated with EDA–CoFe–C [50], HDA–CoFe–C [52], and PANI–FeCo–C [57] catalysts.

8.3.2 Synthesis Conditions

8.3.2.1 Heat Treatment

The active ORR sites in M–N–C catalysts are believed to be formed during the heat-treatment step, with the resulting activity being strongly dependent on the treatment temperature [42]. The optimum heat-treatment temperature depends on the nitrogen

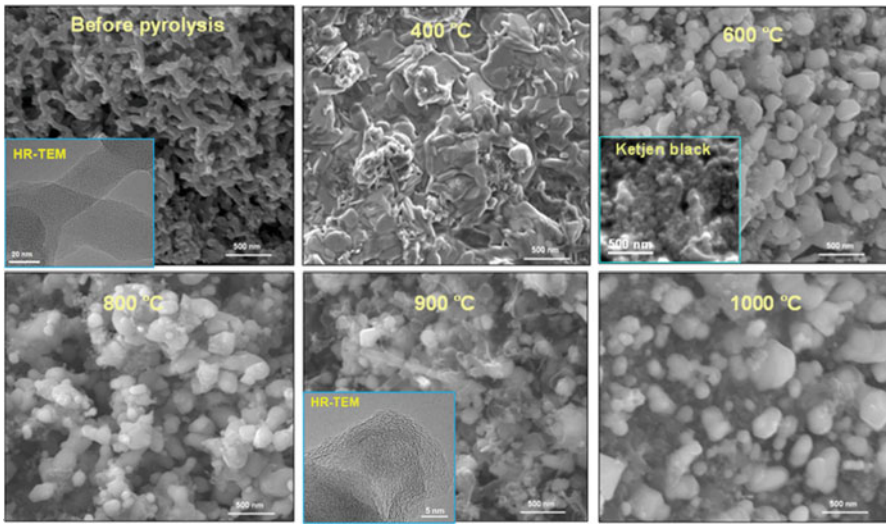

Fig. 8.20 SEM images of PANI–Fe–C catalyst in their final form (after the second heat treatment [43]) as a function of the heat-treatment temperature. Scale bar for all SEM images is 500 nm; scale bar for the HR–TEM inset in the "Before pyrolysis" image is 20 nm; scale bar in the "900 °C" image is 5 nm (reproduced from ref. [43] by permission of The Royal Society of Chemistry)

and transition metal precursors used [22, 42]. It typically falls in the 800–1,100 °C range, sufficient for nitrogen doping into the (partially) graphitized carbon structure. Higher heat-treatment temperatures result in a significant decrease in the number of nitrogen functionalities and reduction in the surface area. For example, the ORR activity of PANI-derived Fe–N–C catalysts has been found to gradually increase with the heat-treatment temperature in the 400–900 °C temperature range and decrease at higher temperatures. The type of carbon nanostructures and catalyst morphology formed during heat treatment at different temperatures may be the factors determining the catalyst performance.

As shown in Fig. 8.20 for PANI-derived Fe–N–C catalysts, the characteristic PANI nanofibers gradually disappear as the heat-treatment temperature increases to 400 °C and the spherical particles begin to form at 600 °C [43]. A higher degree of graphitization is observed at 900 °C, resulting in the formation of graphitic shells often covering sulfide-rich particles (cf. TEM images in Fig. 8.18). Following heat treatment at even higher temperatures, the catalyst morphology becomes highly nonuniform, the particles agglomerate reaching sizes much larger than those in the carbon black originally used in the synthesis, and the surface area significantly decreases. These changes in the carbon structure and morphology, together with their impact on the catalyst ORR performance, point to the importance of the metal-catalyzed transformation of the precursors into new carbon forms in NPMCs.

The effect of heat-treatment temperature on the ORR activity and selectivity of M–N–C catalysts was studied with physical characterization techniques [43]. A correlation between the ORR performance and the BET surface area of a

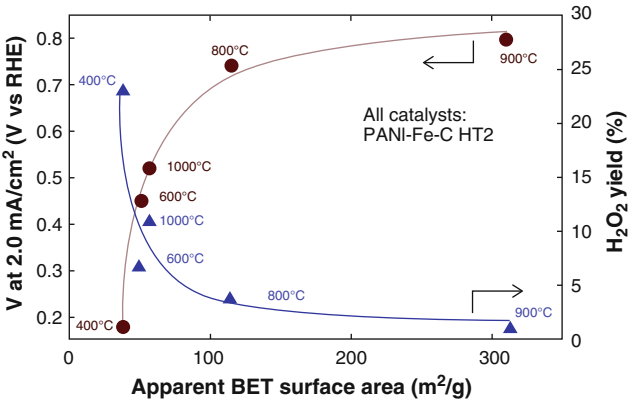

Fig. 8.21 Dependence of the ORR activity and H_2O_2 yield on the BET surface area of a PANI–Fe–C catalyst heat-treated at temperatures ranging from 400 to 1,000 °C (reproduced from ref. [43] by permission of The Royal Society of Chemistry)

PANI–Fe–C catalyst is shown in Fig. 8.21. The surface area increases from ~40 $m^2\ g^{-1}$ for the catalyst heat-treated at 400 °C to ~300 $m^2\ g^{-1}$ for the catalyst treated at 900 °C, before dropping to ~60 $m^2\ g^{-1}$ for the catalyst heat-treated at 1,000 °C [43].

Also dependent on the heat-treatment temperature are the content and relative ratios of different nitrogen functionalities in M–N–C catalysts. An increase in the heat-treatment temperature from 600 to 1,000 °C leads to a decrease in the total nitrogen content but without a significant change in the ORR activity [43]. Those changes are accompanied by an increase in the ratio of quaternary to pyridinic nitrogen [43, 60], suggesting that the ORR activity may not be dependent on the total amount of incorporated nitrogen but on how nitrogen is incorporated into doped nitrogen–carbon hybrid nanostructures. A similar trend was found for Co-based catalysts and TiO_2-supported Fe catalysts [60, 69]. Although pyridinic nitrogen has been often linked to the oxygen reduction activity of NPMC catalysts [46], the quaternary nitrogen content and C–N_x structure distribution, reflected by the ratio of the quaternary to pyridinic nitrogen, appear to play an important role, too [66]. In some cases, an increase in the heat-treatment temperature leads to a decrease in the total nitrogen content and increase in ORR activity. Presently, there is no clear correlation between the absolute content of quaternary or pyridinic nitrogen and the associated active-site density [43].

8.3.2.2 Post-treatment

While ORR active sites are formed during the first heat treatment of NPMC precursors [42], the post-treatment, including the acid leach and the second heat treatment in neutral gas atmosphere (N_2), was shown to be important for the final performance of non-precious metal catalysts [43]. The acid leach results in much

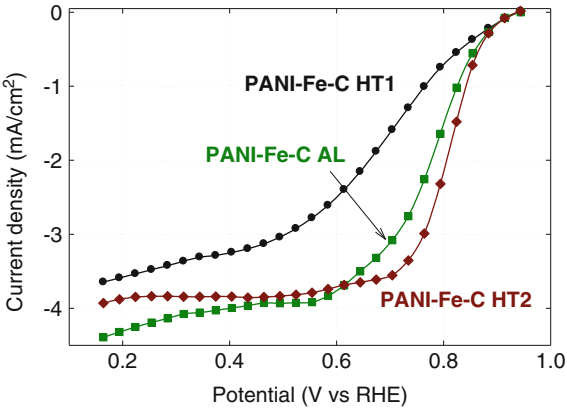

Fig. 8.22 Steady-state ORR polarization plots for PANI–Fe–C catalyst after the first heat treatment at 900 °C (HT1), after the acid leach (AL), and after the second heat treatment at 900 °C (HT2). RDE data in 0.5 M H_2SO_4 at 25 °C. Disk rotation rate: 900 rpm (reproduced from ref. [43] by permission of The Royal Society of Chemistry)

higher ORR activity, thanks to the removal of unstable and unreactive phases from the porous catalyst, which likely leads to an exposure of additional active sites [56]. In the case of a PANI-derived catalyst in Fig. 8.22, the acid leach does not affect the onset ORR potential, indicating no change to the active site. The second heat treatment (after the acid leach) results in further ORR performance improvement. Once again, the onset ORR potential does not change. This implies that neither the acid leach nor the second heat treatment influence the type of active sites present in the catalyst.

It is worth noting that the second heat treatment at 900 °C results in a decrease in the BET surface area (390 vs. 315 $m^2\ g^{-1}$) [43], implying that an increase in the active-site density during the second heat treatment likely offsets the surface area loss. Catalysts with much enhanced ORR activity after the second heat treatment were also demonstrated by Koslowski et al. [70]. The use of reactive gases, especially NH_3, during the second heat treatment was required to generate very significant ORR activity, as previously shown by Fournier et al. [71].

8.3.3 Structure–Property Correlation

M–N–C catalysts are obtained by simultaneously heat-treating precursors of nitrogen, carbon, and transition metal(s) at 700–1,000 °C. The activity and durability of these catalysts greatly depend on the selection of precursors and synthesis chemistry and correlate quite well with the catalyst nanostructure. Although no rational design of active and durable M–N–C catalysts based on a rigorous description of the ORR active site can yet be proposed, some guiding information for the synthesis of future NPMCs is available. It first and foremost stems from the understanding of the effect of nitrogen doping and in situ graphitization of carbonaceous materials in the catalysts.

Various types of nitrogen functionalities, in particular pyridinic and quaternary nitrogen, can be viewed as an n-type dopant of carbon in M–N–C catalysts that can assist in the formation of nanostructures and donate electrons to the carbon [46].

The N–C groups likely behave as one kind of ORR active sites. At the same time, as already stated above, the ORR activity is not governed by the total amount of nitrogen imbedded into the carbon but depends more on how the nitrogen is incorporated into the nitrogen–carbon hybrid nanostructures [43]. The nature of N–C groups in M–N–C catalysts can be controlled by tuning the synthesis conditions, usually aimed at maximizing catalytic activity [43]. Regardless of the nitrogen precursor used, XPS data indicate a higher content of the quaternary nitrogen in Fe–N–C catalysts than in Co–N–C catalysts. This indicates that, in the presence of Fe, nitrogen atoms are likely to be also incorporated in the interior rather than at the edges of the graphene layer.

Apart from possibly participating in the active site, the transition metal in M–N–C catalysts appears to be linked to the formation of new carbon structures by catalyzing graphitization of nitrogen–carbon precursors [46]. The highly graphitic carbon nanostructures may serve as a matrix for the ORR-active nitrogen and/or metal moieties. NPMC research to date suggests that the presence of graphitized carbon phase in some ORR catalysts may play a role in enhancing their stability. Also, the formation of different carbon nanostructures strongly depends on the type of nitrogen precursor, transition metal, heat-treatment temperature, and support used in the catalysts synthesis [43, 52, 60, 72], which can all be correlated to the catalyst performance. Compared to catalysts obtained from other nitrogen precursors, in situ formed nitrogen-doped graphene sheets are particularly abundant in the PANI–Co–C catalyst [57], the effect that may be responsible for an enhanced catalytic activity of the catalyst. Graphene-sheet structures were found not to be as common in Co-based catalysts synthesized using other nitrogen–carbon precursors, such as EDA [50], HDA [52], and cyanamide [48]. The morphology of the HDA–Co–C catalyst is dominated by carbon nanostructures different from graphene sheets, e.g., onion-like carbon nanoshells, which are not particularly ORR active. Well-defined graphitized carbon shells surrounding metal-rich particles were also observed in catalysts derived from Fe(III) tetramethoxyphenyl porphyrin chloride (FeTMPP-Cl), at a relatively high heat-treatment temperature of 1,000 °C. The graphite-shell formation was correlated to an increase in the open cell potential of the catalysts in oxygen-saturated solutions [73]. The significant morphological differences between Fe- and Co-based catalysts possibly attest to the strong effect of the transition metal precursor selection on carbon/nitrogen structures during the heat treatment. It seems that Co is a more effective catalyst of the carbonization process at high temperatures, leading to highly graphitic carbon structures [43]. Although Co appears to facilitate the formation of graphitized carbon structures, potentially helping the catalyst performance, the Co-based catalysts are generally less ORR-active in acid media than the Fe-based ones. This is probably due to the difference in the nature of the ORR active sites formed in the presence of different transition metals. Binary-metal catalysts, involving both Co and Fe, seem to benefit from the unique Co-induced graphene-rich morphology and highly active sites, created in the presence and/or participation of Fe. That unique combination of the two functions has led to catalysts with high ORR activity and, at the same time, improved stability [42].

Carbon nanostructures ex situ introduced into the NPMC may also play a role in improving catalytic activity and durability. Very recently, a highly active and durable NPMC was prepared based on nanotube–graphene (NT–G) complexes treated in NH_3 at 900 °C [74]. The abundance of edges and defect sites was claimed to be responsible for the high ORR activity. The high degree of graphitization of carbon nanotubes, the exfoliation of the outer walls, and the presence of graphene flakes in NT–G could impart high oxidative corrosion resistance of the catalytic sites. The NT–G catalyst showed a significant loss in activity on exposure to cyanide anions, suggesting that high ORR activity stems from iron-containing catalytic sites. Aberration-corrected scanning transmission electron microscopy (STEM) and electron energy loss spectrum (EELS) mapping techniques on the atomic scale revealed the presence of iron atoms on the edges of graphene sheets in close proximity to nitrogen species [74].

8.3.4 Beyond Standard PEFC Cathodes

8.3.4.1 Alkaline Fuel Cells

Alkaline fuel cells present several potential advantages over their acidic counterparts, dominating low-temperature fuel cell applications today. Main advantages include performance improvements and cost reduction, both associated with the use of NPMCs.

Thanks to the −59 mV change in the potential per every pH unit, the operation potential of an ORR catalyst is expected to be by ca. −0.83 V lower in a 1.0 M solution of a strong base than in 1.0 M solution of a strong acid. Such a potential shift impacts the double-layer structure and the electric field at the electrode–electrolyte interface, altering the adsorption strength of neutral species [76]. Decreased anionic adsorption in alkaline media is expected to help the kinetics of electrocatalytic reactions, including the ORR [77]. While improvements in the electrocatalysis can be significant, the better materials stability afforded by the use of alkaline electrolytes is even more important. In particular, a wide variety of NPMCs have shown comparable corrosion resistance in alkaline media to that of precious metals, which makes them particularly suitable for alkaline fuel cells [76].

The presence of nitrogen-doped graphitic carbon has been considered necessary for an efficient multi-electron transfer in the ORR catalysis in alkaline media [78]. An EDA-derived binary CoFe catalyst, heat-treated at 900 °C and acid-leached in 0.5 M H_2SO_4 at 80 °C, was successfully demonstrated in an anion exchange membrane fuel cell (AEMFC) at the University of South Carolina, using an A201 membrane (Tokuyama Corporation, Japan), composed of a hydrocarbon main chain and quaternary ammonium groups as ion-exchange sites [75]. In a fuel cell test, the OCVs were found to be 0.97 and 1.04 V for the EDA–CoFe–C and Pt/C catalysts, respectively. The corresponding maximum power densities were measured at 177 and 196 mW cm^{-2} (Fig. 8.23) [75]. At high potentials, the performance of EDA–CoFe–C was slightly lower than that of Pt/C. At intermediate potentials, both catalysts showed

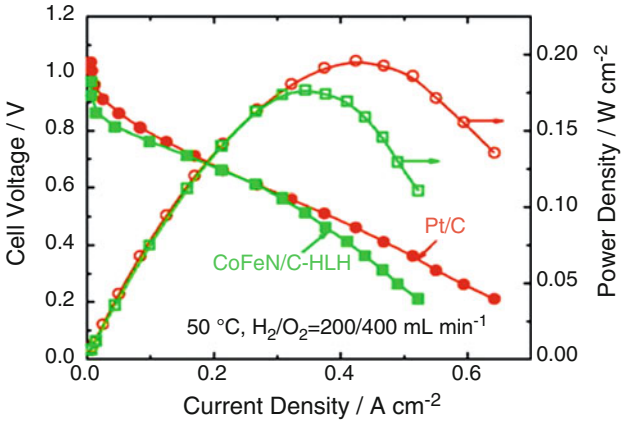

Fig. 8.23 Performance of an H_2–O_2 AEMFC with EDA–CoFe–C and Pt/C cathodes at 50 °C. Cathode catalyst loadings: 4 mg cm^{-2} for EDA–CoFe–C and 0.4 mg_{Pt} cm^{-2} for Pt/C. Anode and cathode gases humidified at 50 °C. Gas flow rates: 200 mL min^{-1} (H_2) and 400 mL min^{-1} (O_2). The A201 membrane thickness 28 μm; ion-exchange capacity 1.8 mmol g^{-1}; conductivity 42 mS cm^{-1} (reprinted from ref. [75] with permission from Elsevier)

very similar activity. The lower performance of EDA–CoFe–C at low potentials may be attributed to high mass transfer and/or ionic resistance in the cathode, caused by a high catalyst loading and considerable thickness of the electrode.

The ORR performance of three different PANI-derived catalysts in an alkaline electrolyte is shown in Fig. 8.24 [79]. The best performing catalyst, PANI–Co–C, containing a large number of Co_9S_8 particles surrounded by nitrogen-doped graphene sheets, shows the activity and performance stability superior to that of a Pt/C reference catalyst. Oxygen is effectively reduced at that catalyst to OH^- in a four-electron reaction mechanism.

8.3.4.2 Methanol Tolerance

Methanol (MeOH) crossover from the anode to the cathode in the direct methanol fuel cell (DMFC) is responsible for significant depolarization of the Pt cathode catalyst. Compared to Pt-based catalysts, NPMCs are poor oxidation catalysts, of methanol oxidation in particular, which makes them highly methanol-tolerant. As shown in Fig. 8.25, the ORR activity of a PANI–Fe–C catalyst in a sulfuric acid solution is virtually independent of the methanol content, up to 5.0 M in MeOH concentration. A significant performance loss is only observed in 17 M MeOH solution (~1:1 water-to-methanol molar ratio), a solution that can no longer be considered aqueous. The changes to oxygen solubility and diffusivity, as well as to the double-layer dielectric environment, are all likely to impact the ORR mechanism and kinetics, which may not be associated with the electrochemical oxidation of methanol at the catalyst surface. Based on the ORR polarization plots recorded at

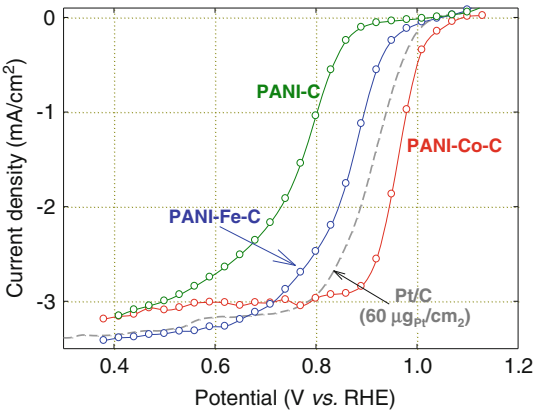

Fig. 8.24 Steady-state ORR polarization plots recorded with three PANI-derived and Pt/C reference catalysts in 0.1 M KOH electrolyte at 25 °C. Polarization data recorded after 1,000 durability cycles in a potential range from 0.6 to 1.0 V vs. RHE in an N_2-saturated solution. RDE rotation rate: 900 rpm (reprinted from ref. [79] with permission from the Electrochemical Society)

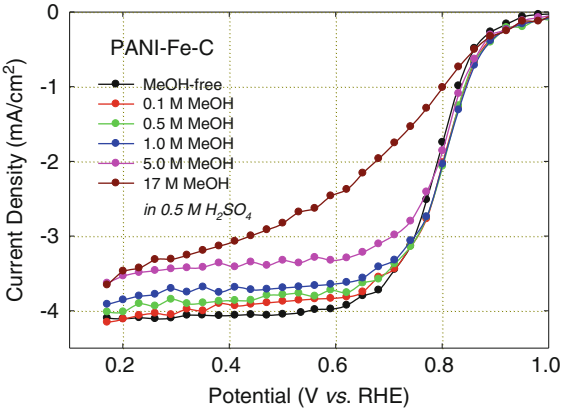

Fig. 8.25 Steady-state ORR polarization plots recorded with a PANI–Fe–C catalyst at an RDE in 0.5 M H_2SO_4 electrolyte at 25 °C and at a rotation speed of 900 rpm as a function of methanol concentration

lower methanol concentrations, the PANI–Fe–C catalyst should be viewed as a potential methanol-tolerant replacement for Pt at the DMFC cathode.

High methanol tolerance of an NPMC was also demonstrated with a heat-treated CoTMPP catalyst [80].

8.3.4.3 Anion Tolerance

A high-temperature (HT) PEFC operating with phosphoric-acid-doped polybenzimidazole (PBI) membrane has several potential advantages over the low-temperature PEFCs utilizing either perfluorosulfonic acid or hydrocarbon membranes. The advantages include faster ORR kinetics at elevated temperatures (150–200 °C), improved CO tolerance, and an ease of the water and heat management [81]. However, the ORR activity of the state-of-the-art Pt catalysts is significantly reduced in HT-PEFCs due to severe poisoning of the catalyst by chemisorbed phosphate ions ($H_2PO_4^-$ and HPO_4^{2-}).

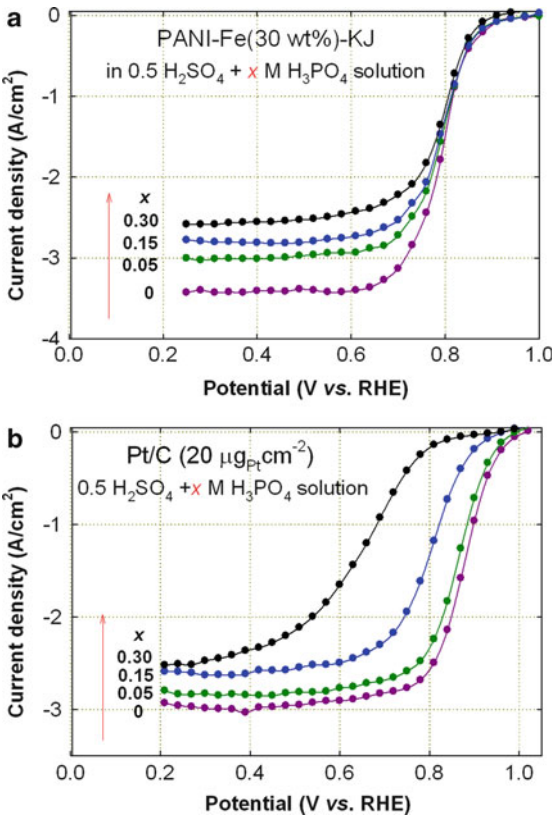

Fig. 8.26 Steady-state ORR polarization plots recorded with (**a**) PANI–Fe(30 wt %)–KJ and (**b**) Pt/C catalyst in 0.5 M H_2SO_4 electrolyte at 25 °C as a function of concentrations of H_3PO_4. RDE rotation rate: 900 rpm

Unlike Pt and Pt alloys, NPMCs do not suffer from the specific adsorption of anions. As shown in Fig. 8.26a, the ORR performance of a PANI–Fe–C catalyst in the kinetic range of the steady-state RDE polarization curves is virtually independent of the solution concentration of H_3PO_4. In the case of a Pt/C catalyst (Fig. 8.26b), a continuous ORR activity loss is observed with an increase in H_3PO_4 concentration due to the chemisorption of phosphate ions. Thanks to their resistance to anions (true also of (bi)sulfate in sulfuric acid solutions), NPMCs represent an attractive alternative to Pt-based catalysts at the HT-PEFC cathode.

8.4 Conclusions

Heat-treated non-precious metal catalysts, synthesized from earth-abundant elements, are capable of catalyzing the ORR and efficiently generating electricity from fuels via a direct electrochemical conversion. Carbon–nitrogen precursors, supports, and in situ formed graphitized carbon play an important role in the catalyst performance.

Advanced catalyst synthesis is likely to focus in the future on (a) novel nitrogen precursors, (b) optimization of the content of transition metal(s) (Fe, Co, and possibly other metals), (c) precursor ratios, (d) functionalization of the catalyst surface (e.g., by NH_3, CO_2, and N_2 treatment), (e) fine-tuning of the heat-treatment conditions (temperature, heating rate, treatment duration, gas atmosphere), and (f) the effect of post-treatment (acid leach, additional heat treatments, etc.). The interaction between the metal and precursors of carbon and nitrogen during the heat treatment will likely be controlled more precisely in the future. The knowledge gained will be used to formulate chemical and morphological requirements for catalysts.

The major challenge of non-precious metal electrocatalysis of oxygen reduction reaction continues to be the lack of knowledge of the active catalytic sites and reaction mechanisms. The difficulties in the identification of the active sites are augmented by the virtual absence of effective NPMC characterization tools for direct probing of the surface of heat-treated catalysts. Further progress in the development of NPMCs will likely depend on the ability to characterize and understand the source(s) of the activity of the catalysts that have been already developed and are under development today.

References

1. Jahnke H, Schoenborn M (1969) Cathodic reduction of oxygen on phthalocyanine-carbon catalysts. Presses Acad Eur: 60–65
2. Kadish KM, Smith KM, Guilard R (eds) (2000) The porphyrin handbook, vol 1, Synthesis and organic chemistry. Academic, Boston
3. Collman JP, Denisevich P, Konai Y, Marrocco M, Koval C, Anson FC (1980) Electrode catalysis of the four-electron reduction of oxygen to water by dicobalt face-to-face porphyrins. J Am Chem Soc 102(19):6027–6036
4. Boulatov R, Collman JP, Shiryaeva IM, Sunderland CJ (2002) Functional analogues of the dioxygen reduction site in cytochrome oxidase: mechanistic aspects and possible effects of CuB. J Am Chem Soc 124:11923–11935
5. Jahnke H, Schoenborn M, Zimmermann G (1973) N4 chelates as catalysts in fuel cells. Thieme: 71–89
6. Berezin BD (1962) Metal phthalocyanines in solution. VI. Effect of the nature of the central ion on the stability of the macroring of phthalocyanine in sulfuric acid solutions. Zh Fiz Khim 36:494–501
7. Tarasevich MR, Radyushkina KA, Andruseva SI (1977) Electrocatalysis of oxygen reduction on organic metallic complexes. Bioelectrochem Bioenerg 4:18–29
8. Collman JP, Ghosh S (2010) Recent applications of a synthetic model of cytochrome c oxidase: beyond functional modeling. Inorg Chem 49:5798–5810
9. Kadish KM, Smith KM, Guilard R (2000) The porphyrin handbook, vol 6, Applications: past, present and future. Academic, New York
10. Jahnke H, Schoenborn M, Zimmermann G (1974) Transition metal chelates as catalysts for fuel cell reactions. Electrochem Soc: 303–318
11. Bagotskii VS, Tarasevich MR, Levina OA, Radyushkina KA, Andruseva SI (1977) Electrocatalysis of the reduction of oxygen on metal chelates in an acid electrolyte. Dokl Akad Nauk SSSR 233:889–891

12. Fuhrmann A, Wiesener K, Iliev I, Gamburzev S, Kaisheva A (1980) Characterization of heat-treated electrocatalytically active tetramethoxyphenylporphyrinatocobalt(II). J Power Sources 6:69–81
13. Wiesener K, Fuhrmann A (1980) Use of tetramethoxyphenylporphyrinatocobalt(II) and its pyrolysis products as catalysts for cathodic oxygen reduction in acidic fuel cells. Z Phys Chem 261:411–424
14. Weng LT, Bertrand P, Lalande G, Dodelet JP (1994) Charaterization of electrocatalysts for oxygen reduction by ToF SIMS. Proceedings of the Int Conf on Sec Ion Mass Spec, Wiley: 442–445
15. Ramaswamy N, Mukerjee S (2010) Electrocatalysis of oxygen reduction on non-precious metallic centers at high pH environments. ECS Trans 33:1777–1785
16. Charreteur F, Jaouen F, Dodelet J-P (2009) Iron porphyrin-based cathode catalysts for PEM fuel cells: influence of pyrolysis gas on activity and stability. Electrochim Acta 54:6622–6630
17. Medard C, Lefevre M, Dodelet JP, Jaouen F, Lindbergh G (2006) Oxygen reduction by Fe-based catalysts in PEM fuel cell conditions: activity and selectivity of the catalysts obtained with two Fe precursors and various carbon supports. Electrochim Acta 51:3202–3213
18. Gupta S, Tryk D, Bae I, Aldred W, Yeager E (1989) Heat-treated polyacrylonitrile-based catalysts for oxygen electroreduction. J Appl Electrochem 19:19–27
19. Yamana M, Darby R, Dhar HP, White RE (1983) Electrodeposition of cobalt tetraazaannulene on graphite electrodes. J Electroanal Chem Interfacial Electrochem 152:261–268
20. Shigehara K, Anson FC (1982) Catalysis of the reduction of dioxygen to water at graphite electrodes coated with two transition metal catalysts acting in series. J Electroanal Chem Interfacial Electrochem 132:107–118
21. Lefèvre M, Proietti E, Jaouen F, Dodelet J-P (2009) Iron-based catalysts with improved oxygen reduction activity in polymer electrolyte fuel cells. Science 324(5923):71–74
22. Chen Z, Higgins D, Yu A, Zhang L, Zhang J (2011) A review on non-precious metal electrocatalysts for PEM fuel cells. Energy Environ Sci 4(9):3167–3192
23. Wiesener K, Ohms D, Neumann V, Franke R (1989) N_4 macrocycles as electrocatalysts for the cathodic reduction of oxygen. Mater Chem Phys 22(3–4):457–461
24. Franke R, Ohms D, Wiesener K (1989) Investigation of the influence of thermal treatment on the properties of carbon materials modified by N_4-chelates for the reduction of oxygen in acidic media. J Electroanal Chem 260(1):63–68
25. Radyushkina KA, Tarasevich MR (1986) Electrocatalytic properties of pyropolymers based on N_4 complexes. Elektrokhimiya 22:1155–1170
26. Dhar HP, Darby R, Young VY, White RE (1985) The effect of heat treatment atmospheres on the electrocatalytic activity of cobalt tetraazaannulenes: preliminary results. Electrochim Acta 30(4):423–429
27. Meng H, Larouche N, Lefevre M, Jaouen F, Stansfield B, Dodelet J-P (2010) Iron porphyrin-based cathode catalysts for polymer electrolyte membrane fuel cells: effect of NH_3 and Ar mixtures as pyrolysis gases on catalytic activity and stability. Electrochim Acta 55:6450–6461
28. Kadish KM, Smith KM, Guilard R (eds) (2000) The porphyrin handbook, vol 9, Database of redox potentials and binding constants. Academic, New York
29. Jahnke H, Schonborn M, Zimmermann G (1976) Organic dyestuffs as catalysts for fuel cells. Top Curr Chem 61:133–181
30. van Veen JAR, van Baar JF, Kroese KJ (1981) Effect of heat treatment on the performance of carbon-supported transition-metal chelates in the electrochemical reduction of oxygen. J Chem Soc Faraday Trans 1: Pys Chem in Cond Phases 77(11):2827–2843
31. Nabae Y, Moriya S, Matsubayashi K, Lyth SM, Malon M, Wu L, Islam NM, Koshigoe Y, Kuroki S, Kakimoto M-a, Miyata S, Ozaki J-i (2010) The role of Fe species in the pyrolysis of Fe phthalocyanine and phenolic resin for preparation of carbon-based cathode catalysts. Carbon 48(9):2613–2624
32. Serov A, Robson MH, Halevi B, Artyushkova K, Atanassov P (2012) Highly active and durable templated non-PGM cathode catalysts derived from iron and aminoantipyrine. Electrochem Commun 22(1):53–56

33. Huang H-C, Shown I, Chang S-T, Hsu H-C, Du H-Y, Kuo M-C, Wong K-T, Wang S-F, Wang C-H, Chen L-C, Chen K-H (2012) Pyrolyzed cobalt corrole as a potential non-precious catalyst for fuel cells. Adv Func Mater 22(16):3500–3508
34. Beck F, Dammert W, Heiss J, Hiller H, Polster R (1973) Electrocatalysis of the oxygen cathode by metal-phthalocyanines and -dibenzotetraazaannulenes. Z Naturforsch Teil A 28: 1009–1021
35. Alt H, Binder H, Sandstede G (1973) Mechanism of the electrocatalytic reduction of oxygen on metal chelates. J Catal 28:8–19
36. Van Veen JAR, Van Baar JF, Kroese KJ (1981) Effect of heat treatment on the performance of carbon-supported transition metal chelates in the electrochemical reduction of oxygen. J Chem Soc Faraday Trans 1(77):2827–2843
37. Van Wingerden B, Van Veen JAR, Mensch CTJ (1988) An extended x-ray absorption fine structure study of heat-treated cobalt porphyrin catalysts supported on active carbon. J Chem Soc Faraday Trans 1(84):65–74
38. Fuhrhop JH (1975) Irreversible reactions at the porphyrin periphery (excluding photochemistry). Porphyrins Metalloporphyrins: 625–666
39. Vallejos-Burgos F, Utsumi S, Hattori Y, García X, Gordon AL, Kanoh H, Kaneko K, Radovic LR (2012) Pyrolyzed phthalocyanines as surrogate carbon catalysts: initial insights into oxygen-transfer mechanisms. Fuel 99(1):106–117
40. Yamanaka I, Onizawa T, Suzuki H, Hanaizumi N, Nishimura N, Takenaka S (2012) Study of direct synthesis of hydrogen peroxide acid solutions at a heat-treated MnCl-porphyrin/activated carbon cathode from H_2 and O_2. J Phys Chem C 116:4572–4583
41. Schulenburg H, Stankov S, Schünemann V, Radnik J, Dorbandt I, Fiechter S, Bogdanoff P, Tributsch H (2003) Catalysts for the oxygen reduction from heat-treated iron(III) tetramethoxyphenylporphyrin chloride: structure and stability of active sites. J Phys Chem B 107(34): 9034–9041
42. Jaouen F, Proietti E, Lefevre M, Chenitz R, Dodelet J-P, Wu G, Chung HT, Johnston CM, Zelenay P (2011) Recent advances in non-precious metal catalysis for oxygen-reduction reaction in polymer electrolyte fuel cells. Energy Environ Sci 4(1):114–130
43. Wu G, Johnston CM, Mack NH, Artyushkova K, Ferrandon M, Nelson M, Lezama-Pacheco JS, Conradson SD, More KL, Myers DJ, Zelenay P (2011) Synthesis-structure-performance correlation for polyaniline-Me-C non-precious metal cathode catalysts for oxygen reduction in fuel cells. J Mater Chem 21(30):11392–11405
44. Jaouen F, Herranz J, Lefèvre M, Dodelet J-P, Kramm UI, Herrmann I, Bogdanoff P, Maruyama J, Nagaoka T, Garsuch A, Dahn JR, Olson T, Pylypenko S, Atanassov P, Ustinov EA (2009) Cross-laboratory experimental study of non-noble-metal electrocatalysts for the oxygen reduction reaction. ACS Appl Mater Interfaces 1(8):1623–1639
45. Pels JR, Kapteijn F, Moulijn JA, Zhu Q, Thomas KM (1995) Evolution of nitrogen functionalities in carbonaceous materials during pyrolysis. Carbon 33(11):1641–1653
46. Matter PH, Zhang L, Ozkan US (2006) The role of nanostructure in nitrogen-containing carbon catalysts for the oxygen reduction reaction. J Catal 239(1):83–96
47. Biddinger EJ, von Deak D, Ozkan US (2009) Nitrogen-containing carbon nanostructures as oxygen-reduction catalysts. Top Catal 52(11):1566–1574
48. Chung HT, Johnston CM, Artyushkova K, Ferrandon M, Myers DJ, Zelenay P (2010) Cyanamide-derived non-precious metal catalyst for oxygen reduction. Electrochem Commun 12(12):1792–1795
49. Chung HT, Johnston CM, Zelenay P (2009) Synthesis and evaluation of heat-treated, cyanamide-derived non-precious catalysts for oxygen reduction. ECS Trans 25(1):485–492
50. Nallathambi V, Lee J-W, Kumaraguru SP, Wu G, Popov BN (2008) Development of high performance carbon composite catalyst for oxygen reduction reaction in PEM Proton Exchange Membrane fuel cells. J Power Sources 183(1):34–42
51. Subramanian NP, Kumaraguru SP, Colon-Mercado H, Kim H, Popov BN, Black T, Chen DA (2006) Studies on Co-based catalysts supported on modified carbon substrates for PEMFC cathodes. J Power Sources 157(1):56–63

52. Wu G, Dai CS, Wang DL, Li DY, Li N (2010) Nitrogen-doped magnetic onion-like carbon as support for Pt particles in a hybrid cathode catalyst for fuel cells. J Mater Chem 20(15): 3059–3068
53. Wu G, Nelson M, Ma SG, Meng H, Cui GF, Shen PK (2011) Synthesis of nitrogen-doped onion-like carbon and its use in carbon-based CoFe binary non-precious-metal catalysts for oxygen-reduction. Carbon 49(12):3972–3982
54. Wood TE, Tan Z, Schmoeckel AK, O'Neill D, Atanasoski R (2008) Non-precious metal oxygen reduction catalyst for PEM fuel cells based on nitroaniline precursor. J Power Sources 178(2):510–516
55. Nallathambi V, Leonard N, Kothandaraman R, Barton SC (2011) Nitrogen precursor effects in iron-nitrogen-carbon oxygen reduction catalysts. Electrochem Solid State Lett 14(6):B55–B58
56. Wu G, Chen ZW, Artyushkova K, Garzon FH, Zelenay P (2008) Polyaniline-derived non-precious catalyst for the polymer electrolyte fuel cell cathode. ECS Trans 16(2):159–170
57. Wu G, More KL, Johnston CM, Zelenay P (2011) High-performance electrocatalysts for oxygen reduction derived from polyaniline, iron, and cobalt. Science 332(6028):443–447
58. Byon HR, Suntivich J, Shao-Horn Y (2011) Graphene-based non-noble-metal catalysts for oxygen reduction reaction in acid. Chem Mater 23(15):3421–3428
59. Gasteiger HA, Kocha SS, Sompalli B, Wagner FT (2005) Activity benchmarks and requirements for Pt, Pt-alloy, and non-Pt oxygen reduction catalysts for PEMFCs. Appl Catal B Environ 56(1–2):9–35
60. Wu G, Nelson MA, Mack NH, Ma SG, Sekhar P, Garzon FH, Zelenay P (2010) Titanium dioxide-supported non-precious metal oxygen reduction electrocatalyst. Chem Commun 46(40): 7489–7491
61. Subramanian NP, Li XG, Nallathambi V, Kumaraguru SP, Colon-Mercado H, Wu G, Lee JW, Popov BN (2009) Nitrogen-modified carbon-based catalysts for oxygen reduction reaction in polymer electrolyte membrane fuel cells. J Power Sources 188(1):38–44
62. Bezerra CWB, Zhang L, Liu H, Lee K, Marques ALB, Marques EP, Wang H, Zhang J (2007) A review of heat-treatment effects on activity and stability of PEM fuel cell catalysts for oxygen reduction reaction. J Power Sources 173(2):891–908
63. Bezerra CWB, Zhang L, Lee K, Liu H, Marques ALB, Marques EP, Wang H, Zhang J (2008) A review of Fe–N/C and Co–N/C catalysts for the oxygen reduction reaction. Electrochim Acta 53(15):4937–4951
64. Ohms D, Herzog S, Franke R, Neumann V, Wiesener K, Gamburcev S, Kaisheva A, Iliev I (1992) Influence of metal ions on the electrocatalytic oxygen reduction of carbon materials prepared from pyrolyzed polyacrylonitrile. J Power Sources 38(3):327–334
65. Lefevre M, Proietti E, Jaouen F, Dodelet JP (2009) Iron-based catalysts with improved oxygen reduction activity in polymer electrolyte fuel cells. Science 324(5923):71–74
66. Ferrandon M, Kropf AJ, Myers DJ, Artyushkova K, Kramm UI, Bogdanoff P, Wu G, Johnston CM, Zelenay P (2012) Multi-technique characterization of a polyaniline-iron-carbon oxygen reduction catalyst. J Phys Chem C 116(30):16001–16013
67. Coutanceau C, Croissant MJ, Napporn T, Lamy C (2000) Electrocatalytic reduction of dioxygen at platinum particles dispersed in a polyaniline film. Electrochim Acta 46(4):579–588
68. Wu G, Li L, Xu B-Q (2004) Effect of electrochemical polarization of PtRu/C catalysts on methanol electrooxidation. Electrochim Acta 50(1):1–10
69. Wu G, Mack NH, Gao W, Ma S, Zhong R, Han J, Baldwin JK, Zelenay P (2012) Nitrogen-doped graphene-rich catalysts derived from heteroatom polymers for oxygen reduction in nonaqueous lithium–O_2 battery cathodes. ACS Nano 6(11):9764–9776
70. Koslowski U, Herrmann I, Bogdanoff P, Barkschat C, Fiechter S, Iwata N, Takahashi H, Nishikori H (2008) Evaluation and analysis of PEM-FC performance using non-platinum cathode catalysts based on pyrolysed Fe- and Co-porphyrins – influence of a secondary heat-treatment. ECS Trans 13(17):125–141
71. Fournier J, Lalande G, Côté R, Guay D, Dodelet JP (1997) Activation of various Fe-based precursors on carbon black and graphite supports to obtain catalysts for the reduction of oxygen in fuel cells. J Electrochem Soc 144(1):218–226

72. Wu G, More KL, Xu P, Wang H-L, Ferrandon M, Kropf AJ, Myers D, Johnston CM, Zelenay P (2013) Carbon-Nanotube-Supported Graphene-Rich Non-Precious Metal Catalyst of Oxygen Reduction with Enhanced Performance Durability. Chem Commun doi: 10.1039/C3CC39121C
73. Gojkovic SL, Gupta S, Savinell RF (1998) Heat-treated iron(III) tetramethoxyphenyl porphyrin supported on high-area carbon as an electrocatalyst for oxygen reduction. J Electrochem Soc 145(10):3493–3499
74. Li Y, Zhou W, Wang H, Xie L, Liang Y, Wei F, Idrobo J-C, Pennycook SJ, Dai H (2012) An oxygen reduction electrocatalyst based on carbon nanotube-graphene complexes. Nat Nanotechnol 7(6):394–400
75. Spendelow JS, Wieckowski A (2007) Electrocatalysis of oxygen reduction and small alcohol oxidation in alkaline media. Phys Chem Chem Phys 9(21):2654–2675
76. Marković NM, Ross PN Jr (2002) Surface science studies of model fuel cell electrocatalysts. Surf Sci Rep 45(4–6):117–229
77. Gong KP, Du F, Xia ZH, Durstock M, Dai LM (2009) Nitrogen-doped carbon nanotube arrays with high electrocatalytic activity for oxygen reduction. Science 323(5915):760–764
78. Li X, Popov BN, Kawahara T, Yanagi H (2011) Non-precious metal catalysts synthesized from precursors of carbon, nitrogen, and transition metal for oxygen reduction in alkaline fuel cells. J Power Sources 196(4):1717–1722
79. Wu G, Chung HT, Nelson M, Artyushkova K, More KL, Johnston CM, Zelenay P (2011) Graphene-enriched Co_9S_8-N-C non-precious metal catalyst for oxygen reduction in alkaline media. ECS Trans 41(1):1709–1717
80. Piela B, Olson TS, Atanassov P, Zelenay P (2010) Highly methanol-tolerant non-precious metal cathode catalysts for direct methanol fuel cell. Electrochim Acta 55(26):7615–7621
81. Lee KS, Yoo SJ, Ahn D, Kim SK, Hwang SJ, Sung YE, Kim HJ, Cho E, Henkensmeier D, Lim TH, Jang JH (2011) Phosphate adsorption and its effect on oxygen reduction reaction for Pt(x)Co(y) alloy and Au(core)-Pt(shell) electrocatalysts. Electrochim Acta 56(24):8802–8810